*Korean J. Chem. Eng.*, 34(2), 539-546 (2017)
DOI: 10.1007/s11814-016-0279-z

pISSN: 0256-1115
eISSN: 1975-7220

# Water vapor permeability, morphological properties, and optical properties of variably hydrolyzed poly(vinyl alcohol)/linear low-density polyethylene composite films

**Ki Seob Hwang*, Hyuk Jun Kwon**, and Jun-Young Lee*,†**

*Korea Institute of Industrial Technology, 89 Yangdaegiro-gil, Ipjang-myeon, Seobuk-gu, Cheonan-si, Chungcheongnam-do 31056, Korea
**Department of Chemical Engineering, Yonsei University, 134 Shinchon-dong, Seodaemoon-gu, Seoul 03722, Korea
(*Received 30 January 2016 • accepted 11 October 2016*)

**Abstract**−Poly(vinyl alcohol) (PVA)/linear low-density polyethylene (LLDPE) composite films were prepared using PVAs of various molecular weights and degrees of hydrolysis. The crystallinity, water permeability, mechanical properties, and optical properties of the composite films were analyzed based on the absorption properties of the different PVAs. The formation of the composite film became increasingly difficult with increase in the molecular weight and the degree of hydrolysis of PVA, because the resulting crystallinity increased the intramolecular hydrogen bonding of the hydroxyl groups on the main chains of PVA. The 4-98/LLDPE composite film absorbed water gradually and continuously for a long time, and its water vapor absorption rate was similar to that of the 4-88/LLDPE film but lower than that of the PVA 205/LLDPE film. The mechanical properties of the 4-98/LLDPE film were slightly better than those of the 4-88/LLDPE film but inferior to those of the PVA 205/LLDPE film.

Keywords: PVA/LLDPE Composite Films, Water Vapor Permeability, Optical Transmittance, Hydrolysis, Water Vapor Absorption

## INTRODUCTION

The industrial applications of composite materials have significantly increased owing to their superior properties compared to those of conventional isotropic materials. Composite materials exhibit high strength weight and stiffness-weight ratios, corrosion resistance and thermal stability, and are well suited for use in structures in which the weight is a fundamental variable in the design process [1]. Polymer composites are increasingly being utilized for automotive, aerospace, energy, packaging, and flame-retardant applications [2].

Recently, studies for improving the water vapor permeability of films have been carried out using composites of poly(vinyl alcohol) (PVA), polyolefin, and other materials [2-6]. In these studies, some compounded PVA and water-barrier materials [2,3], while others used additives to create good dispersions in polyolefin matrices [4-6].

PVA is prepared by the hydrolysis of poly(vinyl acetate). PVA becomes increasingly water-soluble and hydrophilic as the degree of hydrolysis increases to 80-90%. This increases the biocompatibility and the non-toxicity, permitting the use of PVA in biodegradable polymers [5,7-10]. Therefore, PVA has been extensively used as a controlled drug-release hydrogel, a membrane material for chemical separations, and as a barrier membrane for food packaging [11]. However, PVA film exhibits poor mechanical properties and thermal stability [12], as well as limited processability, compatibility, and degradability [13], restricting the use of the PVA film for heavy-duty applications. It is difficult to produce PVA films using melting processes because the melting and the decomposition temperatures of PVA are similar [14,15]. Therefore, the production of PVA films is limited to wet-processing using water as a solvent, which requires high energy consumption and dissolution time, and additional drying processes [16]. To overcome the problems associated with the processability and the physical properties of PVA, it is frequently combined with polyolefin and additional fillers.

In this study, composite films of linear low-density polyethylene (LLDPE) and PVAs with different molecular weights and degrees of hydrolysis were prepared. The water vapor transmission rate, morphology, and optical properties of the composite films were analyzed.

## EXPERIMENTAL

### 1. Materials

LLDPE was obtained from Hanhwa Chemical Co. (3224 grade, Melt Index value ASTM D1238 2.0 g/10 min). The PVA grades, Mowiol® 4-88, 8-88, 18-88, 4-98, 10-98, 20-98 (Sigma-Aldrich) and PVA 205 (Kuraray) were used to prepare the composite films with LLDPE. The information characterizing the PVAs is shown in Table 1. The molecular weight of PVA 205 was determined by gas permeation chromatography (GPC) analysis. To facilitate the compounding between PVA and LLDPE, zinc stearate (Sinwon Chemicals) and PE wax (Korea Petrochemical) were employed.

### 2. Preparation of PVA/LLDPE Composite and Film

The PVA granules were pulverized using a ball mill and sieved with a 74 mesh and used for further experiments. The PVA constituted 10% of the total composition in each LLDPE film. For each composite film, 180 g of each PVA and 1,500 g of LLDPE were used.

†To whom correspondence should be addressed.
E-mail: jaylee@kitech.re.kr

**Table 1. The molecular weight, degree of hydrolysis and viscosity of PVAs**

| Grade | Mw | Hydrolysis | Viscosity | Polymerization | Manufacturer |
|---|---|---|---|---|---|
| PVA205 | 41,526[a] | 86.5-89.0 | 4.6-5.4 | 847[b] | Kuraray |
| 4-88 | 31,000 | 86.7-88.7 | 3.5-4.5 | 630 | Mowiol® |
| 8-88 | 67,000 | 86.7-88.7 | 7.0-9.0 | 1,400 | |
| 18-88 | 130,000 | 86.7-88.7 | 16.0-20.0 | 2,700 | |
| 4-98 | 27,000 | 98.0-98.8 | 4.0-5.0 | 600 | |
| 10-98 | 61,000 | 98.0-98.8 | 9.0-11.0 | 1,400 | |
| 20-98 | 125,000 | 98.0-98.8 | 18.5-21.5 | 2,800 | |

[a]The molecular weight using GPC (Gel Permeation Chromatography)
[b]Basis on result through GPC, the degree of polymerization were calculated according to ratio vinyl acetate and vinyl alcohol

An activator of 70 g PE wax and a resin stabilizer of 20 g zinc stearate were also added to the mixture.

First, each PVA was added to a Henschel mixer. The mixing was continued until the internal temperature reached 80 °C, and then extrusion was performed using a small twin screw extruder (length/diameter=32 : 1) with a screw diameter of 55 mm. For temperature control, the chamber was set with eight heating zones of different temperatures (150, 150, 150, 150, 155, 160, 170, and 170 °C at the hopper, the six heating chambers, and the die, respectively), and the extrusion was at an average spin rate of 800 rpm. The extruded materials were cooled to temperatures <40 °C using an air fan. The obtained compound was sliced using a cutting machine to samples of 3-4 mm length for pelletization.

The composite film was obtained using the film blowing machine equipped with a 30 mm single screw extruder (length/diameter= 7 : 1). The temperature was controlled by setting four heating zones at 200, 180, 180, and 150 °C. The thickness of the formed film was 150±5 μm.

### 3. Degree of Water Absorption

The degree of water absorption of each PVA composite film was measured after drying at 40 °C for 24 h in a vacuum oven. Samples weighing 5 g were subsequently placed in a chamber maintained at a constant temperature of 70 °C and a relative humidity (RH) of 90% for 7 h, and the change in the weight of the sample was measured after each hour. The water absorption rate was calculated by the following equation:

$$\text{Water absorption rate (g/g)} = \frac{\text{weight of wet sample (g)} - \text{weight of dry sample (g)}}{\text{weight of dry sampel (g)}} \quad (1)$$

### 4. Field Emission-scanning Electron Microscopy

Each PVA-LLDPE composite film was immersed in liquid nitrogen and crushed before being coated with gold for the FE-SEM measurements. The surface morphology and the tomography of the samples were obtained by using a JEOL JSM-6701F field emission-scanning electron microscope (FE-SEM).

### 5. X-ray Diffraction

X-ray diffraction (XRD) measurements of the PVA-LLDPE films before and after water absorption and drying involved using a D8 ADVANCE X-ray diffractometer (Bruker AXS GmbH, Germany). The diffraction patterns were obtained at room temperature in the range $5^{\circ}<2\theta<90^{\circ}$ with a step size of 0.03°.

### 6. Differential Scanning Calorimetry

Differential scanning calorimetry (DSC, DSC Q20, TA Instrument Inc.) analyses used 10-15 mg of the LLDPE film and the PVA-LLDPE composite film. Each sample was heated from room temperature to 100 °C (first heating) at 10 °C/min, held for 5 min at 100 °C, and cooled to −40 °C, before heating again to 200 °C at 10 °C/min while scanning (second heating). The thermal properties, such as the melting point ($T_m$) and the glass transition temperature ($T_g$), were determined from the second heating scan. The relative percentage of the crystalline content ($X_C$) of each sample was calculated according to the equation:

$$X_C = \frac{\Delta H_f}{\Delta H_f^0 \omega} \times 100 \quad (2)$$

Here, $\Delta H_f$ is the heat of fusion of the LLDPE or the composite, $\Delta H_f^0$ is the heat of fusion of 100% crystalline PE ($\Delta H_{100}$=290 J/g) [17,18], and $\omega$ is the mass fraction of the LLDPE in the composite.

### 7. Water Vapor Transmission Rate

The water vapor transmission rate (WVTR) of each sample (size - 5 $cm^2$) was measured by using a permeation test system (MOCON, Permatran-W 3/61) at atmospheric pressure, 37.8 °C, and 100% RH.

### 8. Moisture Content

The moisture content of the PVA-LLDPE composite films was determined with a moisture balance (MA 100H, Sartorius). Using

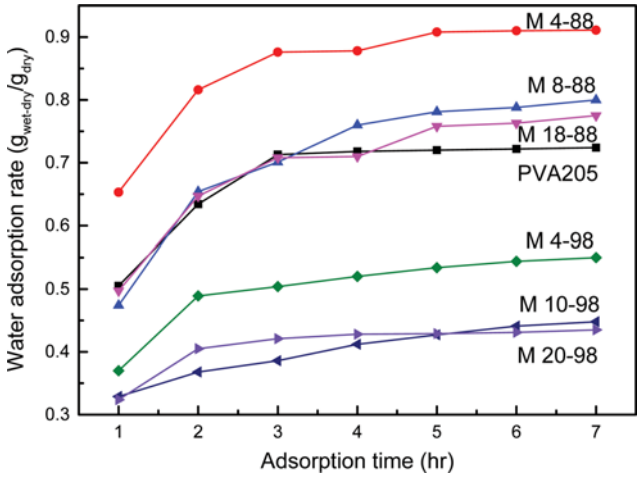


**Fig. 1. Water absorption rate of variably PVAs with times.**

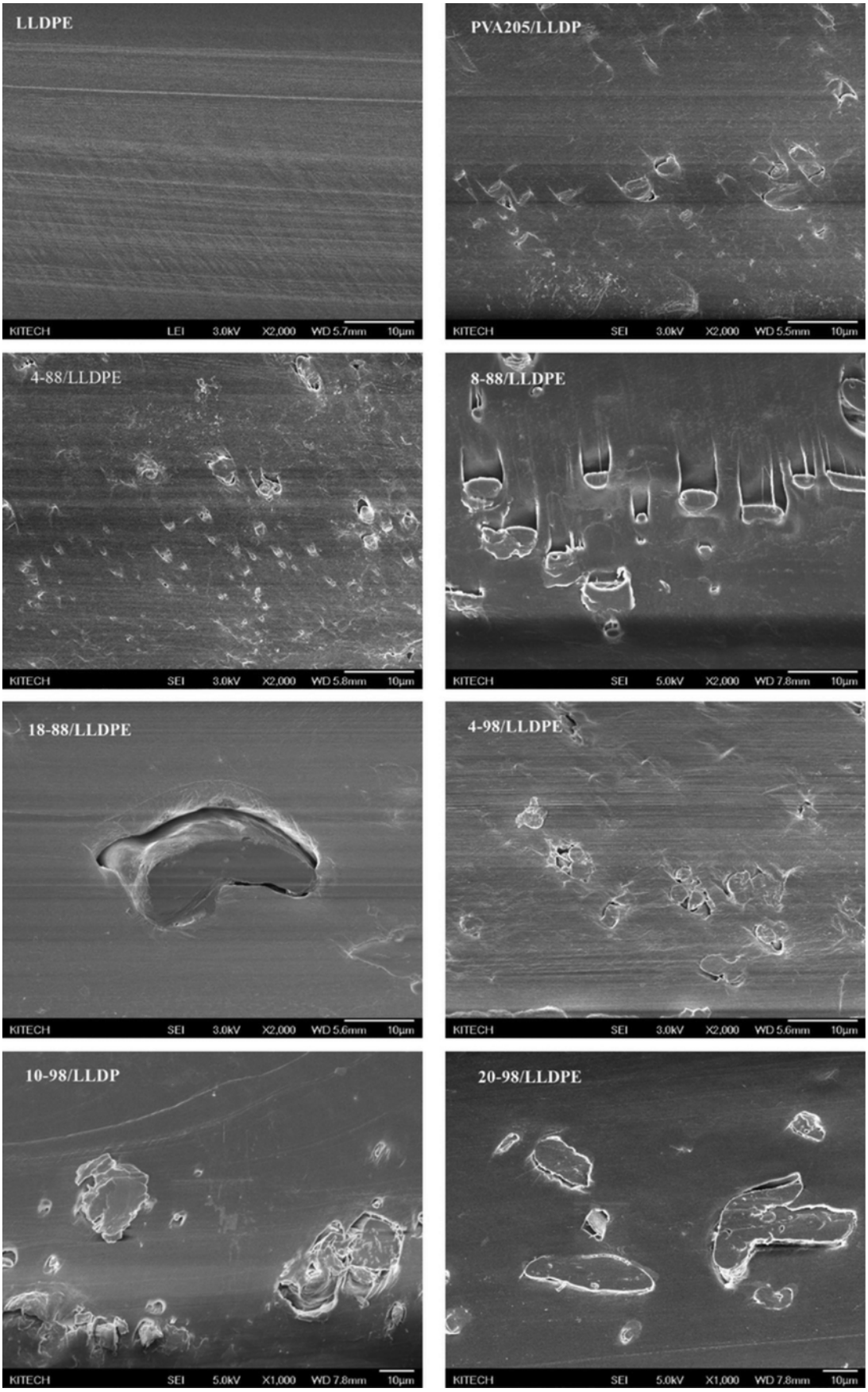


**Fig. 2. Cross-section SEM images of LLDPE and PVA/LLDPE composite films.**

approximately 1 g of the material initially, the weight loss was monitored after heating at 105 °C, until a constant weight was achieved.

**9. Haze and Total Luminous Transmittance**

The haze and the total luminous transmittance of the PVA-LLDPE composite films were measured by a haze meter (HM-150, MURAKAMI). Our testing method followed the guidelines of ASTM D1003 standards [19].

**10. Tensile Strength and Elongation**

The PVA-LLDPE composite film samples were analyzed according to ASTM D882 to measure the tensile strength and the elongation. Each sample was submitted to the QM 100SE quality measurement system (QMESYS Inc.) and tested using a cross-speed of 50 mm/min and a load cell of 200 N. The measurements of tensile strength and elongation were repeated three times and the average values are reported in the present study.

## RESULTS AND DISCUSSION

Generally, the solubility of PVA in water depends on the degree of polymerization and the degree of hydrolysis [20]. Fully hydrolyzed PVA is completely soluble only in boiling water. The partially hydrolyzed grades of PVA are water soluble at room temperature, although the grades with a degree of hydrolysis of 70-80% are soluble in water only at temperatures of 10-40 °C. Above 40 °C, the solution becomes cloudy at a temperature referred to as the cloud point, before precipitating the PVA. The hydroxyl groups in PVA contribute to strong intra- and inter-molecular hydrogen bonding, which reduces the solubility of the compound in water. The presence of residual acetate groups in partially hydrolyzed PVA weakens these hydrogen bonds, permitting solubility at lower temperatures. The degrees of water vapor absorption of the PVA powders with various molecular weights and degrees of hydrolysis are shown in Fig. 1.

4-88 exhibited a degree of water vapor absorption of 0.653 after 1 h, and 0.911 after 7 h; this is the highest value of absorption among the PVA powders. 8-88, 18-88, and PVA 205 showed degrees of water vapor absorption of 0.474, 0.497, and 0.505, respectively, after 1 h, and 0.800, 0.775, and 0.724, respectively, after 7 h. PVA 205 with a similar degree of hydrolysis to those of 8-88 and 18-88 absorbed lesser amount of water vapor. The molecular weight and the $T_g$ of PVA 205 were found to be 41,526 Dalton and 179.8 °C, respectively, using GPC and DSC analyzers. Also, the endothermic peak point (198.2 °C) of PVA 205 was higher than those of 4-88, 8-88 and 18-88, and lower than those of 4-98, 10-98 and 20-98. The increase in the amount of hy- drogen bonding resulted in a lower degree of water vapor absorption of PVA 205 than those of 4-88, 8-88 and 18-88. The degrees of water vapor absorption of 4-98, 10-98, and 20-98 were 0.370, 0.329, and 0.324, respectively, after 1 h and 0.550, 0.448, and 0.435, respectively, after 7 h. Comparing 4-88, 8-88, and 18-88, which exhibit similar degrees of hydrolysis and different molecular weights, 4-88 has the lowest molecular weight and the highest water vapor absorption. Similarly, 4-98 exhibits the highest water vapor absorption when compared with 10-98 and 20-98. Comparison of the PVAs with similar molecular weights and different degrees of hydrolysis (the pairs, 4-88 and 4-98, 8-88 and 10-98, and 18-88 and 20-98), showed that the PVA with a lower degree of hydrolysis exhibits a higher level of absorbed water vapor. This result is consistent with the trends in the quantities of the hydrogen bonds and the hydroxyl groups, similar to the description [20] of the solubility of the PVAs.

The FE-SEM image of each PVA/LLDPE composite film is shown in Fig. 2. In Fig. 2(b), PVA 205 particles of size smaller than 4 μm are observed in the LLDPE matrix. The 4-88/LLDPE composite film shows a similar dispersion with the presence of 4-88 particles smaller than 4 μm in the LLDPE matrix. The 8-88/LLDPE and the 18-88 LLDPE composite films show particles of larger diameter dispersed in the matrix due to the high molecular weight of the PVA. The diameters of the dispersed particles in the 4-98/LLDPE, 10-98/LLDPE, and 20-98 LLDPE composite films show a similar trend. Comparing the PVAs with different degrees of hydrolysis and similar molecular weights, the particles of dispersed PVA are smaller for lower degrees of hydrolysis. PVA melts at temperatures above the melting point in the manufacturing process of the PVA/LLDPE films, and the crystallinity changes according to the degree of hydrogen bonding, which in turn changes with the amount of hydroxyl groups [15,21,22], in the cooling process as described by Mandelkern et al. [21]. Hence, composite film formation from the highly crystalline particles of the PVAs with large molecular weights was difficult. In addition, the agglomerated particles affected the optical transmission and the water vapor permeability of the composite films.

Fig. 3 shows the optical transmission and the surface state of each PVA/LLDPE composite film. For the films formed with PVA 205, 4-88, and 4-98, the letter behind the film is clearly visible. However, regardless of the degree of hydrolysis, the optical transmission of the other PVA/LLDPE films decreases with increase in the molecular weight. In the LLDPE composite films prepared with 18-88, 10-98, and 20-98, PVA particles are observed on the surfaces.

The XRD data were analyzed to determine the crystallinity of the PVA/LLDPE composite films with different molecular weights and degrees of hydrolysis. Fig. 4 shows the XRD scans of the PVA/LLDPE composite films. The broadened background scattering observed in the XRD data of LLDPE suggests an amorphous structure. The XRD pattern of LLDPE also shows typical peaks corresponding to the (110) and (200) crystallographic planes of the orthorhombic form of PE at 21.4° and 23.8°, respectively, superimposed on the amorphous halo [23]. Similar crystalline peaks were reported by Rizzo et al. [24]. The presence of these characteristic crystalline peaks of LLDPE in the composites clearly indicates that the crystalline structure of LLDPE remains unchanged upon compounding with different kinds of PVA. PVA exhibits reflections corresponding to the $(10\bar{1})$, (101), and (200) crystalline planes at 19.4°, 20.1°, and 22.7°, respectively [25-27]. In the displayed XRD patterns of each PVA/LLDPE composite film, the crystalline reflection peaks of PVA overlap with the planes of LLDPE. In addition, the peak corresponding to the $(10\bar{1})$ crystalline plane seems to sharpen as the molecular weight of PVA increases, because the crystallinity increases with the amount of hydroxyl groups present in the main chain of PVA.

The crystallinity of the composite film was found to change after drying and exposure to water vapor for certain periods of time as evident from the post-absorption XRD patterns shown in Fig. 5.

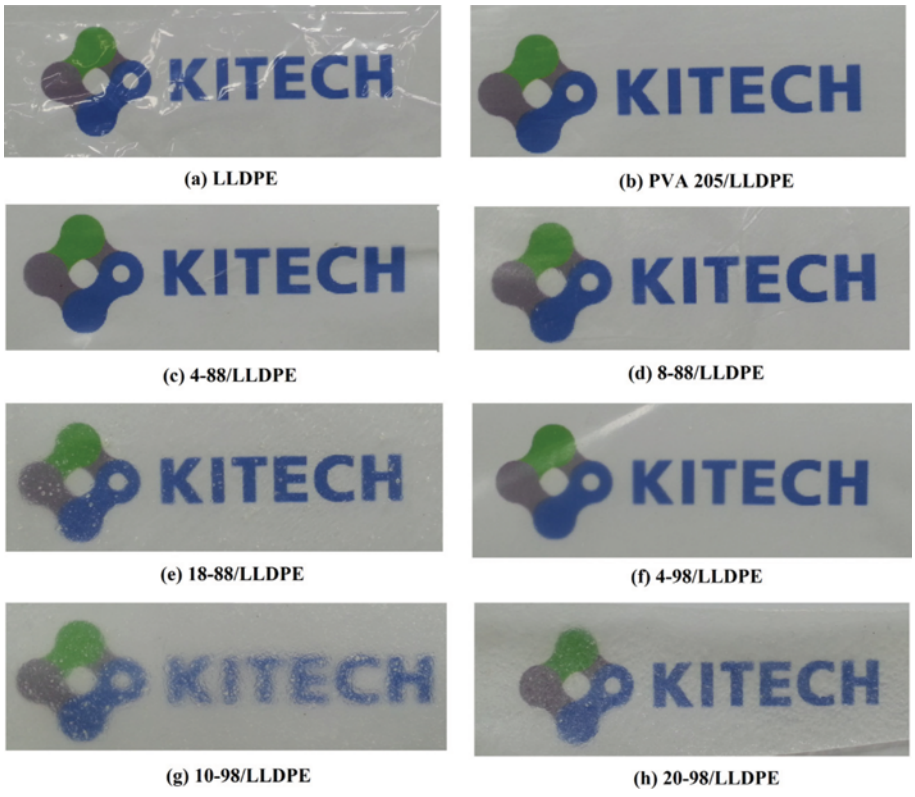


**Fig. 3. Photograph images of the PVA/LLDPE composite films on colorful text.**

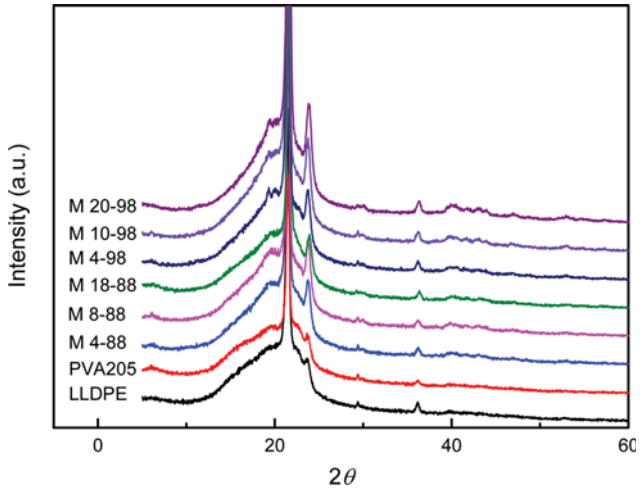


**Fig. 4. X-ray diffraction scans of PVA/LLDPE composite films and the LLDPE film after their producing.**

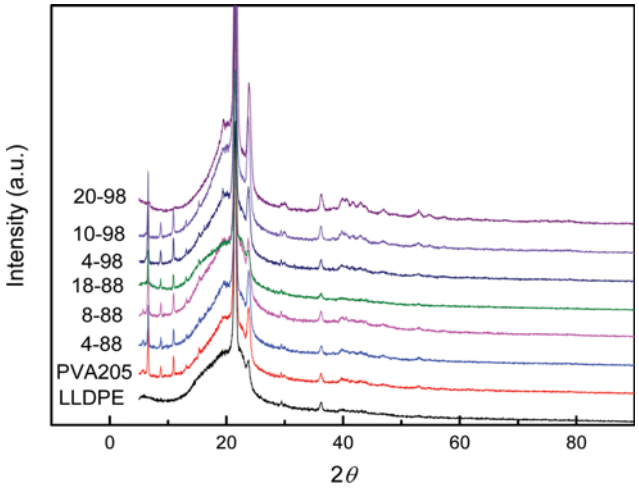


**Fig. 5. X-ray diffraction scans of PVA/LLDPE composite films and the LLDPE film after drying and water vapor adsorption.**

The crystalline planes of the LLDPE films are observed in the post-absorption XRD data as well. However, the XRD data of PVA shows additional sharp peaks at 6.6, 8.7, and 10.9°, and the peak corresponding to the $(10\bar{1})$ plane at 19.5° increases in intensity after water vapor absorption. New peaks corresponding to the (111), $(1\bar{1}1)$, (210), and $(2\bar{1}0)$ planes appear at 39.9°, 40.6°, 41.7°, and 43.1°, respectively, because the crystallinity of the PVAs changes with hydration from the isotactic to the partial atactic and the syndiotactic forms [28].

The degree of crystallinity, Cr, was determined from the integral intensities of the amorphous and crystalline contributions, according to the method of Hermans and Weidinger,

$$\text{Crystallinity (Cr)} = \frac{A_{cr}}{A_{cr} + 2.17A_{am}} \tag{3}$$

$$A_{cr} = A_{total} - 2A_{am}/2 \tag{4}$$

where, $A_{cr}$ is the area of crystalline scattering and $A_{am}$ is the area of

**Table 2. The degree of crystallinity of PVA/LLDPE composite films before and after the drying and adsorption in water vapor using X-ray diffraction method**

| Adsorption | Area | LLDPE | PVA205 | 4-88 | 8-88 | 18-88 | 4-98 | 10-98 | 20-98 |
|---|---|---|---|---|---|---|---|---|---|
| Before | $A_{total}$ | 29301.5 | 21794.0 | 33626.5 | 32797.4 | 28490.1 | 35453.9 | 40478.5 | 42391.8 |
| | $A_{am/2}$ | 9815.9 | 7063.1 | 10392.8 | 9947.00 | 8754.2 | 11089.3 | 11722.0 | 12035.8 |
| | Cr | 0.187 | 0.200 | 0.222 | 0.230 | 0.224 | 0.216 | 0.251 | 0.260 |
| After | $A_{total}$ | 29344.6 | 30281.1 | 31994.9 | 39099.8 | 26795.5 | 35339.5 | 47016.3 | 40489.3 |
| | $A_{am/2}$ | 9807.1 | 8411.9 | 8915.9 | 11673.4 | 8333.5 | 10236.3 | 13478.8 | 10226.4 |
| | Cr | 0.186 | 0.269 | 0.268 | 0.237 | 0.219 | 0.251 | 0.255 | 0.311 |

amorphous scattering. The degree of crystallinity depends strongly on the method of preparation and the technique used for the measurement of the sample [23]. The parameters of the diffraction pattern, i.e., the number of diffraction peaks, their position ($2\theta$) and the width of the diffraction peak are affected upon irradiation of the polymer by different ionizing radiations [29].

The degrees of crystallinity of the various PVA/LLDPE composite films are shown in Table 2. The degrees of crystallinity of the LLDPE film before and after the drying and the adsorption of water vapor are similar. The crystallinity of the PVA/LLDPE composite films before drying and water vapor adsorption increased with increase in the molecular weight and the degree of hydrolysis. The crystallinity of the PVA/LLDPE composite films after the drying and the water vapor absorption was higher than that of the as-prepared films.

The percentage of the crystalline content in the PVA/LLDPE films was obtained from the DSC analysis shown in Fig. 6. The values of the $T_m$ of the composite films were measured at four points during the second heating scan, while those of $T_g$ were measured during the first heating scan. The values of $T_m$ and $T_g$ are shown in Table 3. The results indicate that the $T_g$ and the percentage of crystallinity of the PVA/LLDPE composite films increase with increase in the molecular weight and the degree of hydrolysis of the PVA. The increasing molecular weight and the degree of hydrolysis of PVA in the LLDPE matrix increased because of the number of hydroxyl groups in the main chain; the crystallinity was maintained through strong hydrogen bonding [30-33].

The PVA/LLDPE composite films without holes or agglomerated PVA particles were obtained using PVA 205, 4-88 and 4-98. The WVTRs of these PVA/LLDPE composite films are shown in Fig. 7. The other composite films show the presence of holes and agglomerated PVA particles. The WVTR of the LLDPE film was ~3.7 g/m$^2$·day for the entire duration of the measurement. The WVTR of the PVA 205/LLDPE composite film was maintained at ~2.5 g/m$^2$·day up to 32 h, and then suddenly increased. In the case

**Table 3. The crystallinity of PVA/LLDPE composite films through DSC**

| Sample | 1st Heating | 2nd Heating | | | | | |
|---|---|---|---|---|---|---|---|
| | $T_g$ | $T_{m1}$ | $T_{m2}$ | $T_{m3}$ | $T_{m4}$ | $\Delta H_m$ | $X_c$ |
| LLDPE | 36.3 | 89.1 | 103.9 | 116.2 | 121.9 | 68.9 | 23.8 |
| PVA 205 | 38.7 | 88.6 | 104.0 | 117.5 | 121.9 | 90.8 | 34.8 |
| 4-88 | 39.4 | 90.3 | 104.0 | 117.4 | 121.8 | 88.6 | 27.5 |
| 8-88 | 39.5 | 91.0 | 104.0 | 117.7 | 121.7 | 87.5 | 33.5 |
| 18-88 | 39.7 | 89.1 | 103.9 | 117.3 | 121.9 | 92.6 | 35.5 |
| 4-98 | 41.1 | 88.9 | 103.9 | 116.5 | 121.6 | 90.6 | 34.7 |
| 10-98 | 41.2 | 91.3 | 104.4 | 120.1 | 122.5 | 90.7 | 34.8 |
| 20-98 | 42.1 | 89.6 | 104.3 | 119.3 | 122.3 | 95.1 | 36.4 |

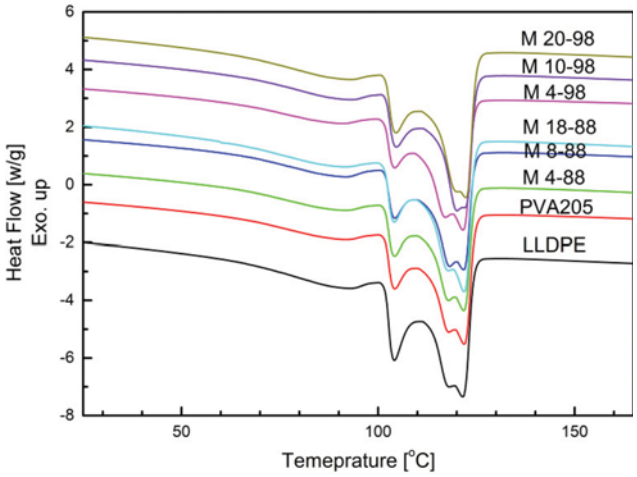


**Fig. 6. DSC 2nd heating scans of PVA/LLDPE composite films and the LLDPE film.**

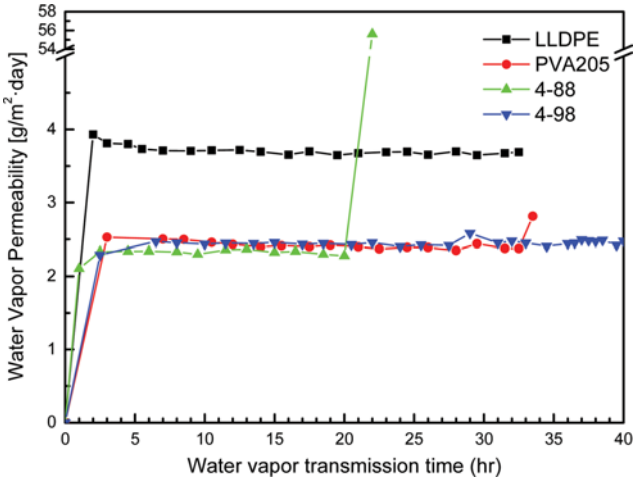


**Fig. 7. Water vapor transmission rate curves of PVA/LLDPE composite films and LLDPE film.**

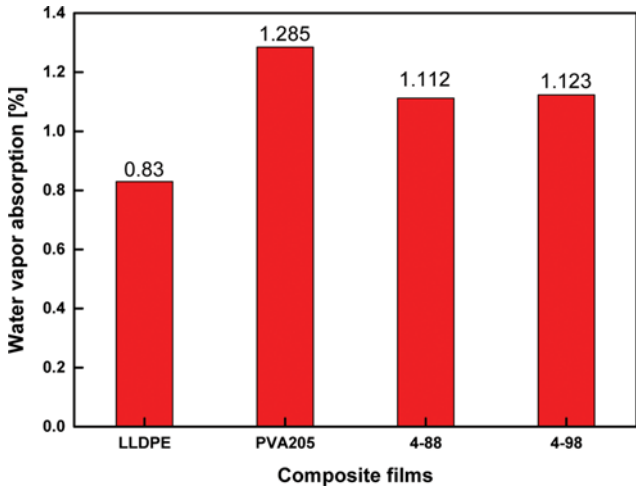


**Fig. 8. Moisture contents of water vapor adsorbed PVA/LLDPE composite films and LLDPE film.**

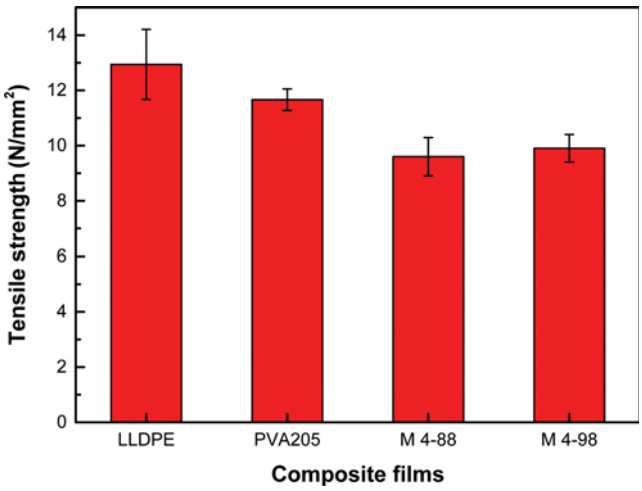


**Fig. 9. Tensile strength at break of PVA/LLDPE composite films and LLDPE film.**

of the 4-88/LLDPE composite film, the WVTR was maintained at ~2.2 g/m$^2$·day for 20 h and later increased. On the other hand, the WVTR of the 4-98/LLDPE composite film was ~2.3 g/m$^2$·day throughout the duration of the measurement. The PVA grades, PVA 205 and 4-88, absorbed water vapor initially, and when the equilibrium between the amount of water vapor absorbed and the water vapor permeability was established, the WVTR increased. The 4-98/LLDPE composite film has a molecular weight like that of the 4-88/LLDPE composite film. Despite a higher degree of hydrolysis and a lower water vapor absorption rate, the 4-98/LLDPE composite film absorbed water for a longer duration.

The plots of water content versus time are shown in Fig. 8. The PVA 205/LLDPE composite film has a relatively higher value while the 4-88 and 4-98/LLDPE composite films exhibit similar values. Although the water vapor permeabilities of the 4-88/LLDPE and the 4-98/LLDPE composite films were similar, it was confirmed through Figs. 7 and 8 that the water vapor absorption rate of the 4-88/LLDPE composite film was higher due to the lower degree of hydrolysis.

The results of the measurements of haze and total luminous transmittance of the LLDPE composite films prepared with PVA 205, 4-88, and 4-98 are shown in Table 4. The value of haze was obtained by using the following equation [34]:

$$T_{Haze} = \left(\frac{T_{Diffuse}}{T_{Total}}\right) \times 100\% \quad (5)$$

The PVA 205/LLDPE composite film shows a relatively high value of haze due to the scattering and diffusion of light by the PVA 205 in the LLDPE matrix. However, the 4-88/LLDPE and the 4-98/LLDPE composite film exhibit relatively lower values of haze, because the dispersed PVA particles were smaller, permitting greater transmission of parallel light. Although the 4-98/LLDPE composite has higher degree of hydrolysis and similar molecular weight compared to those of the 4-88/LLDPE composite film, the higher crystallinity of the films facilitates greater transmission of parallel light. The total luminous transmittance rates of all the PVA/LLDPE composite films were ~90%, similar to that of the LLDPE film.

**Table 4. The optical properties of well-made PVA/LLDPE composite films**

| Sample | Unit | Test method | Haze | Total luminous transmittance |
|---|---|---|---|---|
| LLDPE film | % | ASTM D1003 | 26.9 | 90.0 |
| PVA205/LLDPE film | | | 73.4 | 89.9 |
| 4-88/LLDPE film | | | 18.2 | 90.7 |
| 4-98/LLDPE film | | | 13.9 | 91.3 |

Figs. 9 and 10 show the mechanical properties (tensile strength and elongation) of the LLDPE and the PVA/LLDPE composite films prepared using PVA 205, 4-88, and 4-98. The tensile strength of LLDPE was 12.94±1.27 N/mm$^2$ with 700±62% elongation. In contrast, the tensile strengths of the composite films with PVA 205, 4-88, and 4-98 were obtained as 11.66±0.39, 9.60±0.69, and 9.90±0.50 N/mm$^2$, respectively, and the percentage elongations of these samples were 670±33, 428±32, and 450±62%, respectively. There-

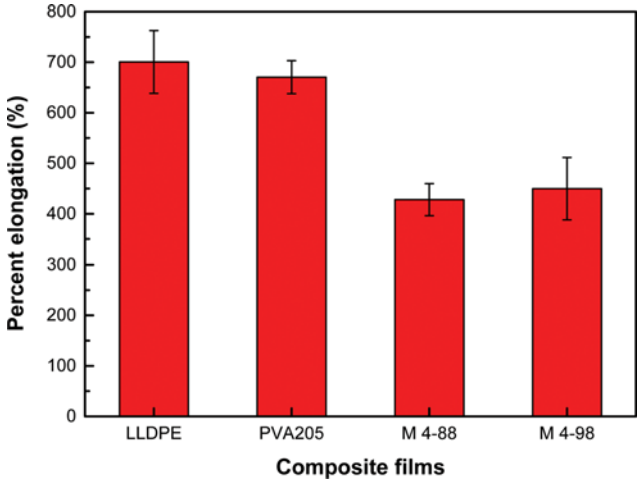


**Fig. 10. Elongation at break of PVA/LLDPE composite films and LLDPE film.**

fore, it can be reasoned that the values of the tensile strength and the percentage elongation were decreased by the addition of PVA to the LLDPE films. This results from the poor interfacial adhesion between the two polymers of different polarities, causing poor stress-transfer between the matrix and the dispersed phase [6,14, 35]. As indicated by the FE-SEM images in Fig. 2, the PVA formed agglomerates due to the strong intra-molecular hydrogen bonds between the hydroxyl groups, which resulted in poor dispersion between the PVA and the LLDPE [14].

## CONCLUSIONS

LLDPE composite films were prepared with PVAs of different molecular weights and degrees of hydrolysis to determine the feasibility of preparing an optically transparent functional film that can act as a water vapor barrier for short durations of ~2 days. Depending on the molecular weight of the PVA, the crystallinity and the polymer interaction were increased by increasing the number of hydroxyl groups in the main chain of the PVA. Increasing the degrees of hydrolysis of the PVAs of similar molecular weights showed the same phenomenon. The formation of the composite film with LLDPE and PVAs of high molecular weights and degrees of hydrolysis was difficult due to the appearance of holes and PVA agglomerates on the surfaces of the films. The PVA/LLDPE composite films were largely amorphous before absorbing water vapor, but the crystallinity increased after drying and absorption of water vapor. The structure of the PVA changed from isotactic to atactic and syndiotactic through the formation of free hydroxyl groups by the absorption of water vapor. The 4-98/LLDPE composite exhibited the best properties in terms of the water vapor transmittance rate, the haze, and the total luminous transmittance rate. In particular, the WVTR of the 4-98/LLDPE composite film was the lowest for the longest period. Hence, these PVA/LLDPE composite films can be used for the packaging of electronic items, powder materials, and food.

## ACKNOWLEDGEMENTS

This study has been conducted with the support of the Korea Institute of Industrial Technology as "Development of Paper Coating Materials for Alternating C8 Perfluoro Chemicals (PFO-Series) (kitech JG-16-0015)".

## SUPPORTING INFORMATION

Additional information as noted in the text. This information is available via the Internet at http://www.springer.com/chemistry/journal/11814.

## REFERENCES

1. S. Oller and E. Oñate, in *Advanced models for finite element analysis of composite materials, 22 pp., Encyclopedia of Composites, 2nd Ed.*, Luigi Nicolais and Assunta Borzacchiello Eds., Wiley, New Jersey, U.S.A. (2013).
2. S. Shori, X. Chen, M. Peralta, H. Gao, H.-C. Zur Loye and H. J. Ploehn, *J. Appl. Polym. Sci.*, **132**, 41867 (2015).
3. D. Kim, J. Jung, S. Park and J. Seo, *J. Appl, Polym. Sci.*, **132**, 41985 (2015).
4. Y. Xianda, W. Anlai and C. Suqin, *Desalination*, **62**, 293 (1987).
5. J. H. Yeun, G. S. Bang, B. J. Park, S. K. Ham and J. H. Chang, *J. Appl. Polym. Sci.*, **101**, 591 (2006).
6. J.-F. Su, Z. Huang, Y.-H. Zhao, X.-Y. Yuan, X.-Y. Wang and M. Li, *Ind. Crops. Prod.*, **31**, 266 (2010).
7. J. Wang, X. Wang, C. Xu, M. Zhang and X. Shang, *Polym Int.*, **60**, 816 (2011).
8. K. E. Strawhecker and E. Manias, *Chem. Mater.*, **12**, 2934 (2000).
9. G. Zhu, F. Wang, Q. Gao, K. Xu and Y. Kiu, *Res. Chem. Intermed.*, Published Online (2013).
10. Y. H. Yu, C. Y. Lin, J. M. Yeh and W. H. Lin, *Polymer*, **44**, 3553 (2003).
11. Q. Deng, J. Li, J. Yang and D. Li, *Composites: Part A*, **67**, 55 (2014).
12. N. Lin, J. Huang, P. R. Chang, D. P. Anderson and J. Yu, *J. Nanomater*, Article ID 573687, 13 (2011).
13. J. Junkasem, R. Rujiravanit and P. Supaphol, *Nanotechnology*, **17**, 4519 (2006).
14. H. Ismail, R. Nordin, Z. Ahmad and A. Rashid, *Iranian Polymer J.*, **19**, 297 (2010).
15. J. Jang and D. K. Lee, *Polymer*, **44**, 8139 (2003).
16. H. M. Kim, J. K. Lee and H. S. Lee, *Thin Solid Films*, **519**, 7766 (2011).
17. K. Hee-Soo, K. Sumin, K. Hyun-Joong and Y. Han-Seung, *Thermochim. Acta*, **451**, 181 (2006).
18. A. S. Luyt and M. J. Hato, *J. Appl. Polym. Sci.*, **95**, 1748 (2005).
19. ASTM D1003-13, ASTM International - Standards Worldwide, http://www.astm.org/ (2013).
20. H. F. Mark, *Encyclopedia of Polymer Science and Technology*, Concise 3rd Ed., Wiley, New Jersey, U.S.A. (2007).
21. C. M. Hassan and N. A. Peppas, *Adv. Polym. Sci.*, **153**, 37 (2000).
22. Y. Nishio, T. Haratani and T. Takahashi, *Macromolecules*, **22**, 2547 (1989).
23. K. A. Moly, H. J. Radusch, R. Androsh, S. S. Bhagawan and S. Thomas, *Euro. Polym. J.*, **41**, 1410 (2005).
24. P. Rizzo, F. Baione, G. Guerra, L. Martinotto and E. Albizzati, *Macromolecules*, **34**, 5175 (2001).
25. H. E. Assender and A. H. Windle, *Polymer*, **39**, 4303 (1998).
26. R. Ricciardi, F. Auriemma, C. De Rosa and F. Lauprétre, *Macromolecules*, **37**, 1921 (2004).
27. K. E. Strawhecker and E. Manias, *Macromolecules*, **34**, 8475(2001).
28. H. E. Assender and A. H. Windle, *Polymer*, **39**, 4295 (1998).
29. Y. Badr, Z. Ali, A. H. Zaharan and R. M. Khafagy, *Polym. Int.*, **49**, 1555 (2000).
30. C. A. Cozzolino, T. O. J. Blomfeldt, F. Nilsson, A. Piga, L. Piergiovanni and S. Farris, *Colloids Surf., A*, **403**, 45 (2012).
31. T. Tanigami, K. Yano, K. Yamaura and S. Matuzawa, *Polymer*, **36**, 2941 (1995).
32. R. M. Hodge, G. H. Edward and G. P. Simon, *Polymer*, **37**, 1371 (1996).
33. R. M. Hodge, T. J. Bastow, G. H. Edward and G. P. Simon, *Macromolecules*, **29**, 8137 (1996).
34. Y. J. Lee, H. S. Park, M. K. Hu, Y. H. Kim, J. J. Park, D. V. Ai, S. Q. Hussain, Y. S. Lee, S. H. Ahn and J. S. Yi, *Energy*, **66**, 20 (2014).
35. H. Y. Choi and Y. S. Lee, *J. Food Eng.*, **116**, 829 (2013).

# Supporting Information

# Water vapor permeability, morphological properties, and optical properties of variably hydrolyzed poly(vinyl alcohol)/linear low-density polyethylene composite films

**Ki Seob Hwang*, Hyuk Jun Kwon**, and Jun-Young Lee*,†**

*Korea Institute of Industrial Technology, 89 Yangdaegiro-gil, Ipjang-myeon, Seobuk-gu, Cheonan-si, Chungcheongnam-do 31056, Korea
**Department of Chemical Engineering, Yonsei University, 134 Shinchon-dong, Seodaemoon-gu, Seoul 03722, Korea
(*Received 30 January 2016 • accepted 11 October 2016*)

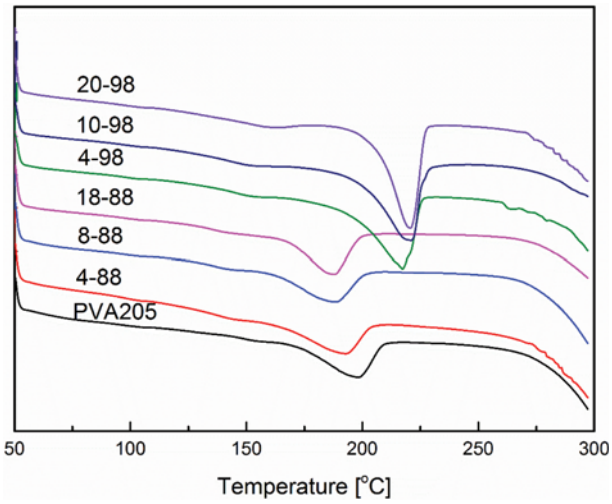


**Fig. S1. DSC curves of various PVA polymers.**

**Table S1. Thermal properties of PVA polymers**

| Sample | Analysis condition | $T_g$ (°C) | Endothermic peak (°C) |
|---|---|---|---|
| PVA205 | 2nd Heating | 149.8 | 198.2 |
| M 4-88 | 2nd Heating | 138.0 | 192.3 |
| M 8-88 | 2nd Heating | 136.4 | 188.1 |
| M 18-88 | 2nd Heating | 134.6 | 188.0 |
| M 4-98 | 2nd Heating | 145.2 | 217.3 |
| M 10-98 | 2nd Heating | 142.0 | 221.0 |
| M 20-98 | 2nd Heating | 151.5 | 220.7 |